DOI:10.2298/CSIS120517013S

# Optimization and Implementation of the Wavelet Based Algorithms for Embedded Biomedical Signal Processing

Radovan Stojanović[1], Saša Knežević[1], Dejan Karadaglić[2], and Goran Devedžić[3]

[1] University of Montenegro, Faculty of Electrical Engineering, Montenegro
stox@ac.me, sasaknezevic@live.com

[2] Glasgow Caledonian University, School of Engineering and Built Environment, UK
Dejan.Karadaglic@gcu.ac.uk

[3] University of Kragujevac, Faculty of Engineering, Serbia
devedzic@kg.ac.rs

**Abstract.** Existing biomedical wavelet based applications exceed the computational, memory and consumption resources of low-complexity embedded systems. In order to make such systems capable to use wavelet transforms, optimization and implementation techniques are proposed. The Real Time QRS Detector and "De-noising" Filter are developed and implemented in 16-bit fixed point microcontroller achieving 800 Hz sampling rate, occupation of less than 500 bytes of data memory, 99.06% detection accuracy, and 1 mW power consumption. By evaluation of the obtained results it is found that the proposed techniques render negligible degradation in detection accuracy of -0.41% and SNR of -2.8%, behind 2-4 times faster calculation, 2 times less memory usage and 5% energy saving. The same approach can be applied with other signals where the embedded implementation of wavelets can be beneficial.

**Keywords:** wavelet transform, microcontroller, QRS, denoising.

## 1. Introduction

The Fourier Transform (FT) is an extremely important and useful tool in signal processing. However since it in its original form treats the global signal in its entirety, it has the drawback that some time-local specific features and peculiarities, especially if they occur rarely, well may be lost in the analysis. This limitation can be partly overcome by the introduction of Short Time Fourier Transform (STFT), which uses a sliding time window of fixed length to localize the analysis in time. Among a number of alternative time–frequency methods, the most promising seems to be the Wavelet Transform (WT) [1]. In contrast to FT, which is restricted to the use of a sinusoid, the WT uses a variety of basic functions, known as wavelets [1]. In its discrete form (DWT),

based on orthogonal wavelet, it is particularly useful in signal compression, detection of local discontinuities, feature extraction, filtering ("de-noising") and other applications [2],[3],[4].

Among others, the DWT has been applied to a wide range of biomedical (BME) signals, including Electrocardiogram (ECG), Electromyogram (EMG), Electroencephalograph (EEG), Photoplethysmograph (PPG), clinical sounds, respiratory patterns, blood pressure trends and DNA sequences [5]. Existing applications perform its calculations off-line using desktop computers or servers with special software or mathematical tools, like MATLAB. The input data are prerecorded in special database such as MIT-BIH, QT, etc, and then later analyzed. Also, data can be imported from memory cards of logger devices, like holters. Such calculations suffer from limited autonomy, bulkiness and obtrusiveness and prevent timely action to the patient.

Recently, a surge in industrial, research and academic interest into telemedicine and home care has been noticed, where low-cost, miniature, telemetry devices overcome the distance barrier between the doctor and patient, e.g. remote vital signs monitors [7], [8]. Such devices are, in fact, Systems on Chip (SoC), consisting of a single Microprocessor/Microcontroller (MC) [9], Programmable Logic Device (PLD) or Application-Specific Integrated Circuit (ASIC). In addition to the sensing, digitalization, data storage, visualization and communication, such chips need to perform real-time signal processing even in time-frequency domain. This is not a trivial task considering the limitations in arithmetic power, memory and power consumption resources.

This paper presents a methodology and techniques to implement WT in low-complexity fixed point embedded architectures, like existing low-cost MCs. The real-time QRS detector and "de-noising" filter are implemented in a 16-bit MC from TI's MSP430 series [6]. For these purposes, the Haar wavelet transform is rewritten from floating point to integer arithmetic. The approach resulted in increased processing speed, minimized memory request and decreased power consumption. The detection accuracy of QRS complexes and signal to noise ratio (SNR) remains on satisfactory level. In addition, the MC is capable to output wavelet and "de-noised" coefficients in the form of analog signal and the RR intervals in the form of digital impulses or in the form of ACSII strings.

The work is organized as following: short introduction on WTs; the proposed optimization techniques; application of WTs in QRS detection and "de-noising" as well as an overview of related work are given in Section 2 and Section 3. Section 4 describes the corresponding hardware and software architectures with associated components and algorithms. The testing procedure and results obtained against qualitative and quantitative criteria are elaborated and discussed in Section 5. The conclusion and references used are enclosed at the end.

## 2. Related Work

In existing literature, there are several contributions on using ASICs and Field Programmable Gate Arrays (FPGAs), which are a type of PLDs, in wavelet-based processing of biomedical signals, and especially ECG. The paper [10] presents QRS detection algorithm implemented in ASIC with 0.18 μm CMOS technology, consuming 176 μW, under 1.8 V supply voltage. The algorithm is based on the Dyadic Wavelet Transform and Multiscale-product Scheme. The algorithm is evaluated on the MIT-BIH database, achieving a high accuracy, >99%. In work [11] the authors propose a structure of QRS detector, which concludes Wavelet Filter Banks and Multi-scale Products to increase detection performances. The filters with Quadratic Spline Wavelet function are chosen to reduce leakage and dynamic power consumption. The design had been prototyped on an Altera's Cyclone-FPGA and synthesized on 0.18 μm Samsung libraries. The paper [12] proposes the algorithm and hardware architecture for QRS detection system based on Mathematical Morphology and Quadratic Spline Wavelet transform, with implementation in Xilinx Virtex™-4SX35 FPGA. The detection accuracy for MIT/BIH arrhythmia database records and resource consumption are reported and seems to be very high. To filter ECG signal and to extract QRS signs the authors in [13] employ the Integer Wavelet Transform. Their system includes several components, which are incorporated in a single FPGA chip from Altera Cyclone Series, achieving sufficient accuracy (about 95%), remarkable noise immunity and low cost.

One of the first references to the introduction of Digital Signal Processors (DSP) in real time processing of ECG signal, by using wavelets, is given in [14]. In particular, QRS complexes, P and T waves are distinguished from noise, baseline drift or artefacts by SPROC-1400 DSP running on 50 MHz. Follow the implementations on modern DSPs, like TI TMS320C6713 [15], where ECG signal is processed in real-time by using DWT and Adaptive Weighting Scheme. An increasing emphasis has been placed in recent years on approaches based on highly integrated, low-power, low-cost MCs like PICs (from Microchip) [16] or MSP430s (from TI). However, their algorithms are still based on traditional methods based on cascade of derivative and averaging filters.

Although much faster, the ASICs and PLDs are more expensive, power demanding, bulky and complicated for rapid prototyping, massive production and maintenance. Thus, the MC remains to be an appropriate solution and a variety of biomedical algorithms, including those WT based, need to be adopted for using in this technology.

# 3. Methodology

## 3.1. WT and DWT

Analytically, the continuous form of WT for a signal *f(t)* is defined by:

$$W(a,b) = \int_{-\infty}^{\infty} f(t)\,\psi_{a,b}(t)dt\,, \tag{1}$$

$$\psi_{a,b}(t) = \frac{1}{\sqrt{a}}\psi^*\left(\frac{t-b}{a}\right), \tag{2}$$

where * denotes complex conjugation and $\psi_{a,b}(t)$ is a window function called the daughter wavelet, $a$ is a scale factor and $b$ is a translation factor. Here, $\psi^*(\frac{t-b}{a})$ is a shifted and scaled version of a mother wavelet $\psi(t)$, which is used as a basis for wavelet decomposition. However, the continuous wavelet transform provides certain amount of redundant information.

Discrete form of WT, known as DWT, is sufficient for most practical applications, providing enough information and offering a significant reduction in the computation time. For a discrete function *f*(*n*), it is given by:

$$W(a,b) = C(j,k) = \textstyle\sum_{n\epsilon Z} f(n)\psi_{j,k}\,(n)\,, \tag{3}$$

where $\psi_{j,k}(n)$ presents a discrete wavelet defined as $\psi_{j,k}(n) = 2^{-\frac{j}{2}}\psi(2^{-j}n - k)$. The parameters $a$, $b$ are defined as $a = 2^j$ and $b = 2^j k$.

In practice, DWT is computed by passing the signal through a Low-Pass ($L_d$) and a High-Pass ($H_d$) filters successively, according to the Mallat's decomposition scheme, Fig. 1 [17]. For each decomposition level *i*, $1 \le i \le N$, the $L_d$ and $H_d$ filters are followed by a downsampling operator, ↓2 expressed as $(X\downarrow 2)[n]=X[2n]$, which is in fact the reduction of a sampling rate by 2. $CA_i(n)$ and $CD_i(n)$ are approximate and detailed coefficients for $i^{th}$ decomposition level. The number of coefficients for $i^{th}$ decomposition level is equal to $l_i$=length($CA_i(n)$)=length($CD_i(n)$)=$length(X(n))/2^i$. The reconstruction consists of upsampling by ↑2 and filtering by filters $L_r$ and $H_r$. The $L_d$, $H_d$, $L_r$, $H_r$ coefficients can vary from the simplest ones like Haar, over Daubechies up to those like Quadratic Spline, having different vector lengths and, usually, floating point interpretation.

The Haar wavelet is considered to be the simplest one with two coefficients per filter:

$$L_d=[1/\sqrt{2},\ 1/\sqrt{2}],\ H_d=[1/\sqrt{2},-1/\sqrt{2}]\,, \tag{4}$$

$$L_r=[\sqrt{2}/2,\sqrt{2}/2]\,,\ \ H_r=[-\sqrt{2}/2,\sqrt{2}/2]\,. \tag{5}$$

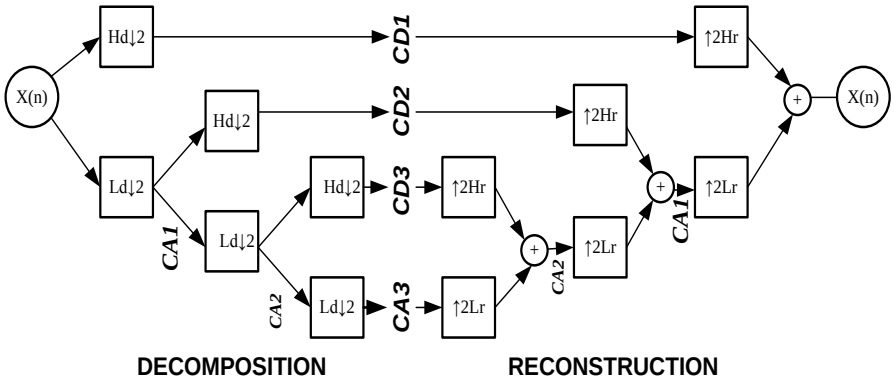


**Fig. 1.** Wavelet decomposition and reconstruction scheme

Haar transform (HT) has a number of advantages; it is (i) conceptually simple, (ii) fast, (iii) memory efficient, since it can be calculated in a place without a temporary array. Also, it is reversible without the edge effect that can be of a problem with some other WTs. But, this transform has several limitations, which can be of a problem in some applications, mainly in signal compression and noise removal from relatively high speed signals like audio or video. But, in the case of biomedical signals this is not an issue.

### 3.2. Integer-Based Optimization

Although very simple in its nature, HT is still complicated for implementation on low-complexity calculation devices like MCs. However, it can be generalized to an integer version. A technique proposed in [18] is in the form of S Transform (ST), whose Forward (FST) and Reverse (RST) versions are defined as:

$$CA_1[n] = \left\lfloor \frac{1}{2}X[2n] + \frac{1}{2}X[2n+1] \right\rfloor , \quad (6)$$

$$CD_1[n] = X[2n] - X[2n+1] , \quad (7)$$

$$X[2n] = CA_1[n] + \left\lfloor \frac{CD_1[n]+1}{2} \right\rfloor , \quad (8)$$

$$X[2n+1] = CA_1[n] - \left\lfloor \frac{CD_1[n]}{2} \right\rfloor , \quad (9)$$

where $\lfloor \ \rfloor$ denotes rounding operator. Because $\left\lfloor \frac{x}{2} \right\rfloor = x \gg 1$, FST and RST can be computed by mere adder-subtractor and shifter, what is, in practice, a key advantage.

### 3.3. WT-Based QRS Detection

WT is capable to distinguish the QRS-complexes within the ECG signal by implementing Mallat's decomposition scheme. $CD_i(n)$ coefficients across the scales show that the peak of the QRS complexes corresponds to the zero crossing (ZC) between two modulus maxima within the coefficients $CD_i(n)$ [19]. Fig. 2 illustrates the decomposition of discrete ECG signal $X(n)$ up to the 4th level, $CD_1(n)$, $CD_2(n)$, $CD_3(n)$ and $CD_4(n)$, by using above defined FST. For each decomposition level, the QRS complex produces two modulus maxima (*min* and *max*) with opposite signs and ZC between, see diagram $CD_4$.

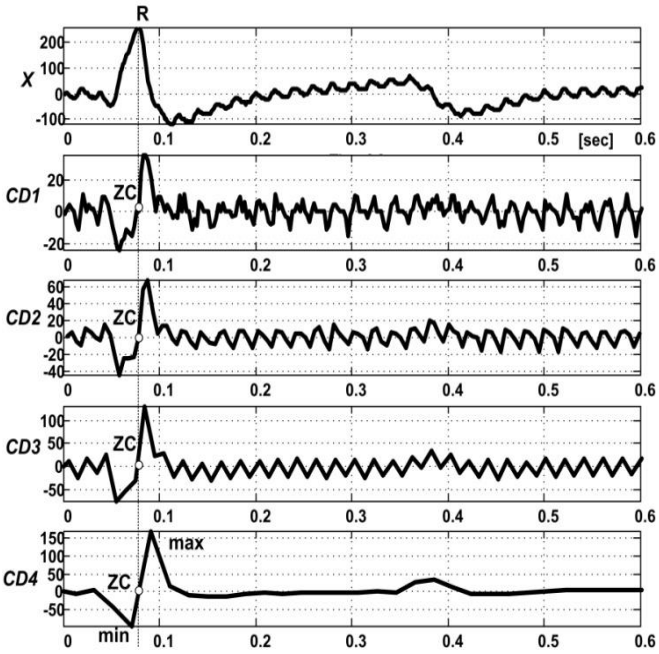


**Fig. 2.** QRS detection using wavelet decomposition based on FST. Signal $X[n]$ is sampled by 800 Hz. $CD_i(n)$ are the details after i[th] decomposition level

The method is very robust and allows direct application over raw ECG data. The frequency domain filtering is performed implicitly by computing the coefficients which is an additional positive feature, very useful in QRS detection. As can be observed, Fig. 2, the original signal becomes practically clear from 4th decomposition level.

Often, the modulus maxima (*min* and *max*) are found by thresholding techniques where the threshold *Tr* varies from one scale to another. For example, the thresholds can be calculated by Root Mean Square (RMS) function, as $Tr$=RMS($CD_i(n)$) for i=1,2 and 3 and $Tr$ =0.5RMS($CD_i(n)$) for i=4, or by Maximum or Mean functions, $Tr$ =MAX($CD_i(n)$) or $Tr$ =MEAN($CD_i(n)$ [19].

In practice, the selection of the most suitable decomposition level/levels is of a challenge. The most of the energy of QRS complex lies between 3 Hz and 40 Hz. Translated to WT, it means somewhere between scales $2^3$ and $2^4$, with the largest at $2^4$. The energy of motion artifacts and baseline wander (i.e. noise) increases for the scales greater than $2^5$. Article [20] states that most energies of a typical QRS-complex are at scales $2^3$ and $2^4$, and the energy at scale $2^3$ is the largest. According to [21], for QRS-complex with high frequency components, the energy at scale $2^2$ is larger than that at scale $2^3$ and authors recommend mainly the scales $2^3$ to $2^4$ for satisfactory detection.

Another complication is the acquisition of certain thresholds for finding the modulus maxima, because the values of thresholds differ, usually, from one level to another. The mentioned restrictions and complications confine the method to off-line use and put heavy demand on the computing resources.

### 3.4. Wavelet-Based Denoising

WT should be effectively used in signal filtering, here known as “de-noising”, especially in the elimination of high frequency and white noise [22]. “De-noising” consists of three successive procedures: decomposition, thresholding and signal reconstruction, Fig. 3a. Firstly, the wavelet transform is derived to a chosen level *N*. Secondly, the detail coefficients from level 1 to *N* are thresholded. Lastly, the original signal is synthesized using the altered detail coefficients from level 1 to *N* and approximation coefficients of level *N*.

There are several methods to define a threshold for the purpose of “de-noising”: global thresholding, where one threshold $T_{hr}$ exists for all samples under consideration and level-based thresholding, where the vector of $2^N$ length, $T_{hr}(1..2^N)$, is used as a threshold [3]. Fig 3b. shows the case of global thresholding applied to the approximation coefficients of $4^{th}$ level and detailed coefficients of $1^{st}$ $2^{nd}$, $3^{rd}$ and $4^{th}$ levels.

From another point of view, thresholding can be either soft or hard [3]. Hard thresholding zeroes out all the values smaller than $T_{hr}$. Soft thresholding does the same thing, and apart from that, subtracts $T_{hr}$ from the values larger than $T_{hr}$. In the contrast to hard thresholding, soft thresholding causes no discontinuities in the resulting signal. Fig. 3b shows the effect of the wavelet-based filtering for ECG signal. The signal *X(n)* is decomposed by FST till $4^{th}$ level, then thresholded by hard threshold $T_{hr}=0.23$ *V* and lastly reconstructed by RST. As can be seen, the reconstructed, filtered, signal *X'(n)* is obtained from only 2.5% of nonzero coefficients.

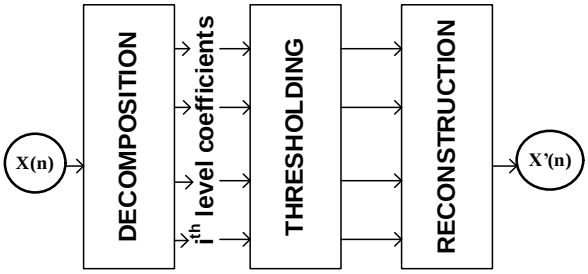


a)

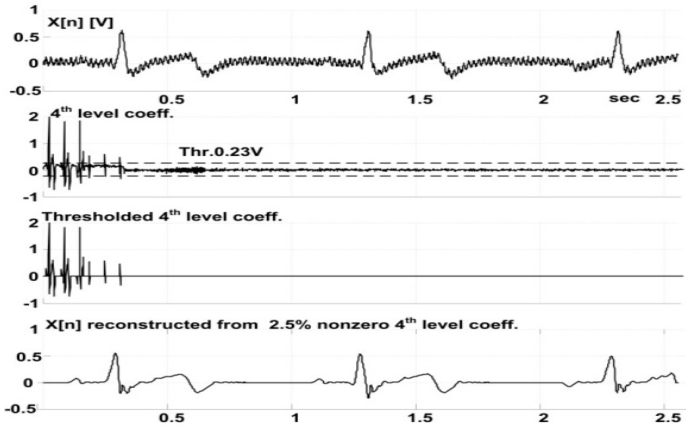


b)

**Fig. 3.** a) Denoising steps, b) Effect on real ECG signal

## 4. Embedded Implementation

For the purpose of biomedical processing, the optimized QRS detection and "de-noising" algorithms are implemented in MSP430F169 microcontroller from MSP430 family, Texas Instruments TI [6]. It is a family of ultralow power microcontrollers optimized for using in portable battery powered devices like medical ones. The MSP430F169 has 16-bit RISC CPU, 16-bit registers, two 16-bit timers, fast 12-bit A/D converter with 8 external input channels, dual 12-bit D/A converter, USART, I2C, DMA, and 48 I/O pins, etc.

On-chip architecture for QRS detection is shown in Fig. 4. The analog ECG signal is fed to the channel A1 of internal ADC. After digitalization and processing in real-time, the output signals are generated in different forms: analog form of details $CD_N(n)$ and $CD_{N-1}(n)$ through the pins P6.6 and P6.7;

pulse form of RR intervals on P1.0 and string (ASCII) form of RR intervals through the USART's TX pin. The RR intervals are distances between QRS complexes, given in ms.

As it is mentioned in Section 2.3, the wavelet decomposition by itself presents a good noise filter used in QRS detection. "De-noising" technique, whose algorithmic steps are elaborated in Section 2, is an additional way to use wavelets as a filter. It is proved, in practice, as very effective tool for signal filtering. Fig. 5 presents wavelet based architecture for "de-noising", implemented in a single MC. The input signal is fed to A1 input of ADC, digitalized, decomposed by FST, thresholded, and finally reconstructed by RST. After reconstruction it is returned to analog form by DAC, see Fig.5 pin P6.7. Overall filtering process is performed in real-time.

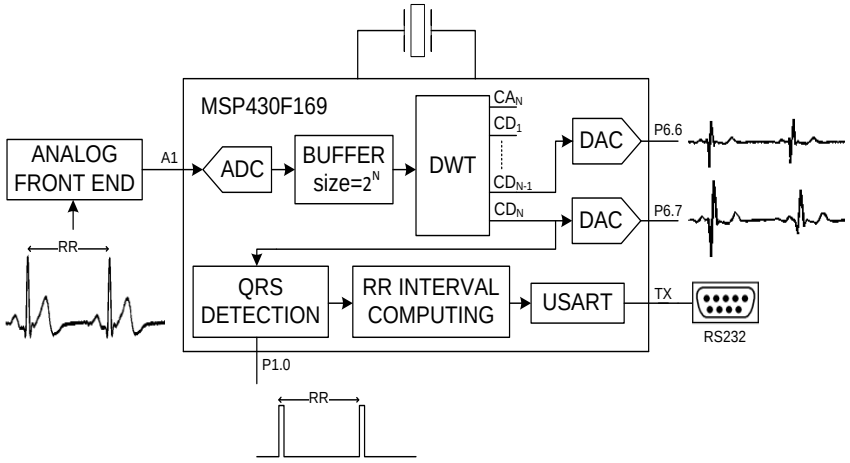


**Fig. 4.** MC architecture for QRS detection

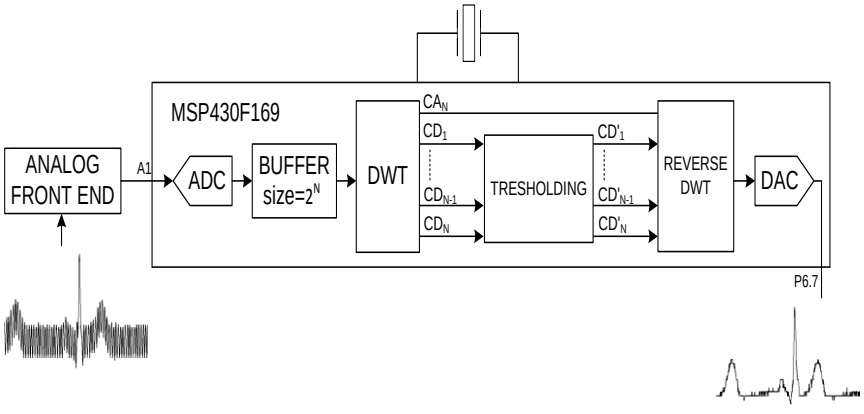


**Fig. 5.** MC architecture for denoising

The real-time implementation of forward and reverse wavelet transform is done through the FST and RST, because of their simplicity and fast calculation. Before processing, the signal is digitalized by 12-bit A/D converter. The sampling frequency is set at 800 Hz for QRS detection and at 762 Hz for denoising. The A/D conversion is performed in an interrupt routine. Between the interrupts, the MSP430 MC uses a low-power operating mode.

In the case of QRS detection, after A/D conversion, each sample is stored in a circular buffer of $2^N$ length, where $N$ represents the number of decomposition levels. When the buffer is filled, the FST is calculated, while the buffer continues to accept new samples. In this research, the decomposition is done till $CD_4(n)$. Then, the $CD_4(n)$ are examined on ZC using negative and positive modulus maxima which are isolated by adaptive thresholding technique. Namely, five successive vectors of 50 $CD_4$ coefficients are examined. For each of them the maximum $M_jmax=max(CD_4(1..50))$ and minimum $M_jmin=min(CD_4(1..50))$ are determined, $M_jmax$, and $M_jmin$, $j=1..5$. Then the negative ($T_1$) and positive ($T_2$) thresholds are defined as:

$$T_1 = \frac{1}{4}\left(\frac{1}{5}\sum_{j=1}^{5} M_j\, min\right), \quad (10)$$

$$T_2 = \frac{1}{4}\left(\frac{1}{5}\sum_{j=1}^{5} M_j\, max\right). \quad (11)$$

Further, the process repeats with values from four old vectors and one new vector. ZC is detected by finding the coefficients associated to the condition $CD_4(n-1)<0$ and $CD_4(n)> 0$.

Detailed algorithm is given in Fig. 6. After computing a new $CD_4$ coefficient, check is performed to see whether that coefficient presents 50$^{th}$ or not? If yes, the $T_1$ and $T_2$ thresholds are set. Then, searching for the negative modulus begins and in case of finding it search for ZC begins. After finding negative modulus and ZC, the algorithm is continuing to search for the positive modulus. If the negative modulus, ZC and the positive modulus are detected successively, then the QRS complex is detected and the algorithm starts to search for a new QRS complex.

In the case of "de-noising", the thresholding is implemented to each decomposition level. The detailed coefficients, whose absolute values are not greater than the threshold, are set to zero. For every decomposition level there is a separate adaptive threshold. For $i^{th}$ (i=1..4) level, ten successive vectors $v$ of $W_i$ (i=1..4) coefficients, $v_{i,j}[1..W_i]$ (i=1..4, j=1..10) are taken in consideration. For each of them, the maximal value $A_{i,j}max=max(v_{i,j}[1..W_i])$ is found and stored in memory. Then, the adaptive threshold for $i^{th}$ level, $T_i$, is calculated as average of the ten maximal values from that level, which is defined as:

$$T_i = \frac{1}{10}\left(\sum_{j=1}^{10} A_{i,j}\, max\right) \quad (12)$$

In order to maintain adaptability of the system for “de-noising”, calculation of the threshold continues with nine old maximal values and one new, which is found within a new vector of $CD_i$ coefficients.

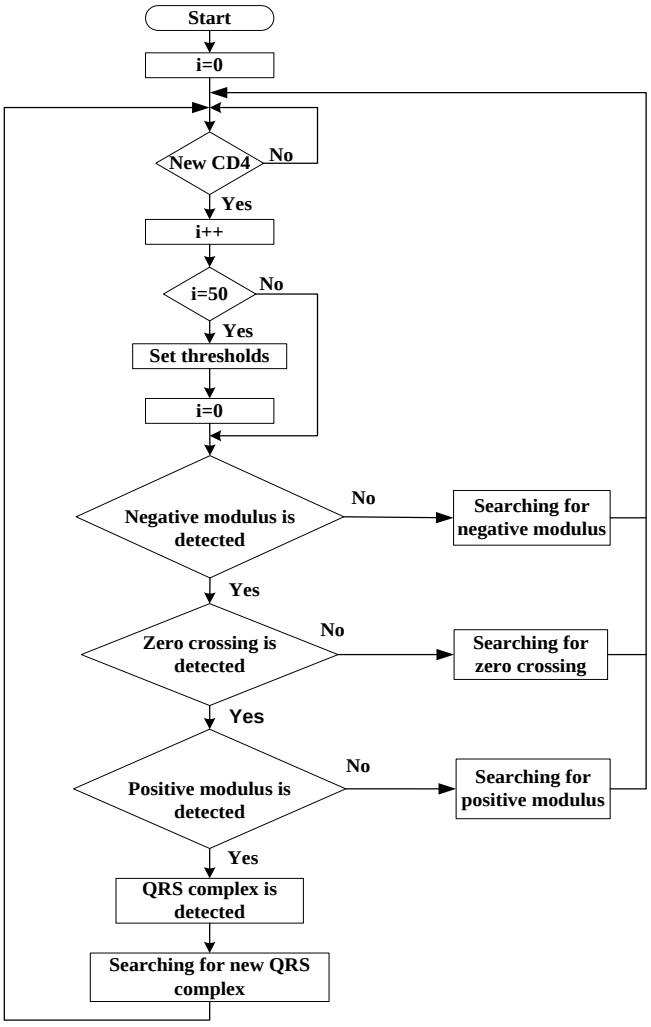


**Fig. 6.** The Algorithm for QRS detection which is implemented on MSP430 MC.

# 5. Results

For purpose of MC implementation and testing, the above presented algorithms for QRS detection and "de-noising" are developed in C code using IAR Embedded Workbench Compiler and then uploaded to MSP430F169 chip, through the Olimex MSP430-P169 development board. The verification of operation and necessary measurements are performed by tool-set consisting of PC, ELVIS II$^+$ NI Platform [23] and digital oscilloscope AGILENT DSO3120A. Designed, LabView Virtual Instrument (VI) read ECG signals from corresponding MIT-BIH files or PPG signals from laboratory files and convert them into analog form via ELVIS II$^+$ platform.

MSP430 chip accepts the emulated signals, performs FST and RST, QRS detection or "de-noising" in real-time. It returns the different analog or digital signals on output pins depending on the running program; $CD_4(n)$ and $CD_3(n)$ in the analog form; RR intervals in pulse (digital) form and RS232 RR intervals in ASCII string form. These signals are observed by oscilloscope or by terminal emulator in case of serial RS232 transmission. Further, the qualitative and quantitative analyses are performed.

## 5.1. Qualitative Analysis

This analysis is mainly performed by on-chip measurements. MC is configured to work in three modes, wavelet decomposition, QRS detector with digital outputs and "de-noising".

In the first mode, the emulated ECG signals are fed to the A/D input A1, digitalized and processed generating analog signals, $CD_3(n)$ *and* $CD_4(n)$ equivalents, on *D/A pins* P6.6 and P6.7, see Fig. 4. Simultaneously, the input and output waveforms are traced by digital oscilloscope. Then, the same ECG signals are processed by MATLAB, off-line, and results are plotted. For illustration, Fig. 7 shows the oscillographs and MATLAB plots of the input ECG signal and corresponding $CD_4(n)$ coefficients. As seen, the waveforms in Fig. 7 b) and Fig. 7 c) match very well. Note that the oscillograph amplitude and time division are printed in legend, bellow waveforms, as example, CH1 200 mV/div, 200.0 ms/div.

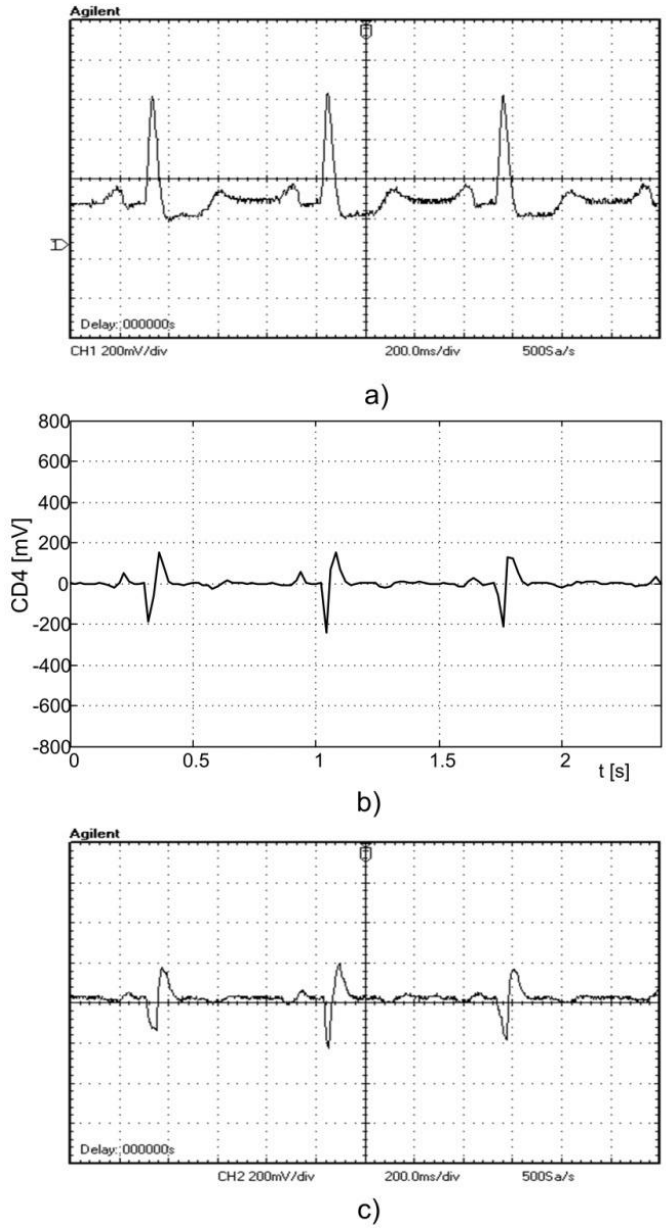


**Fig. 7.** FST calculated by MATLAB, off-line, and by MSP430F169, on-line. a) the oscillograph of the original ECG signal, b) $CD_4(n)$ coefficients plotted by MATLAB, c) oscillograph of $CD_4(n)$ coefficients, recorded on P6.7 pin. The sampling frequency was 800 Hz

In the second mode, the ECG signal is fed to the A/D pin A1, see Fig. 4. The MC performs QRS detection in real time and generates the RR impulses

(pin P1.0), whose positions correspond to the QRS complexes. The time distance between two successive impulses gives a RR interval in ms. Fig. 8 shows the oscillographs of original signal (up) and RR intervals (down). For example, the distance between 1st and 2nd impulse is 580 ms and between 2nd and 3rd is 560 ms that corresponds to the heart rates of 60*1/0.58=103 and 60*1/0.56=107 beats/pm, pm=per minute, indicating an effect of heart rate variability. As can be seen, the generated RR impulses are delayed, shifted, in relation to input signal, for about 50 ms.

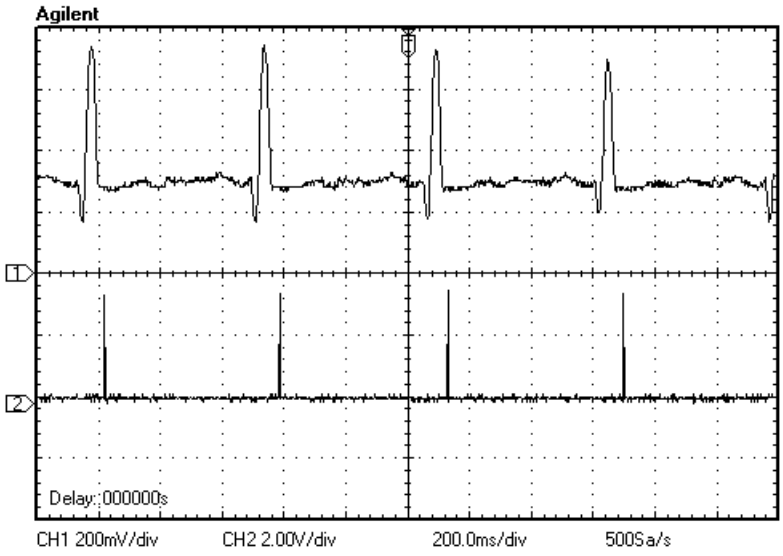


**Fig. 8.** ECG signal with QRS complexes (up) and RR impulses (down) obtained as a result of QRS detection. The sampling frequency was 800 Hz

Third mode is related to real-time “de-noising”, see Fig. 5. Analog forms of ECG and PPG signals, corrupted by 50 Hz or white noise, are fed to the A/D pin A1. The MC digitalize signal, runs “de-noising” code and, in real time, generates the filtered analog signals, D/A pin P6.7. Fig. 9 illustrates the situation with ECG signal corrupted by 50 Hz noise, while Fig. 10 shows filtering results against white noise. Fig. 11 illustrates the case of PPG signal corrupted by 50 Hz noise. The sampling frequency is 762 Hz and filtered signal is delayed for 40 ms. As can be seen, in all cases, the input signals are well filtered after passing “de-noising” code.

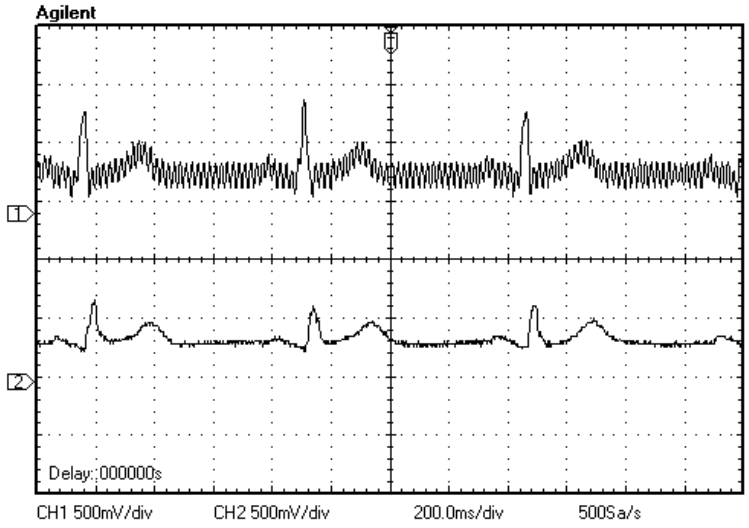


**Fig. 9.** ECG signal corrupted with 50 Hz noise (up) and filtering output (down)

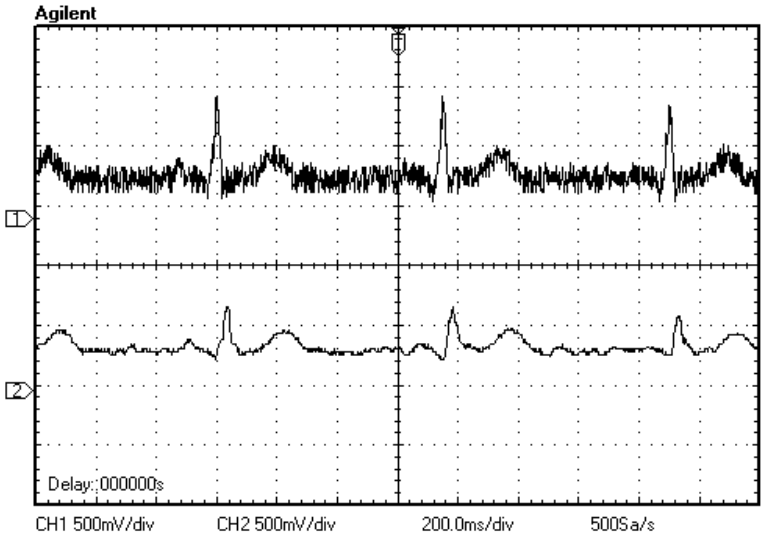


**Fig. 10.** ECG signal corrupted with white noise (up) and filtering output (down)

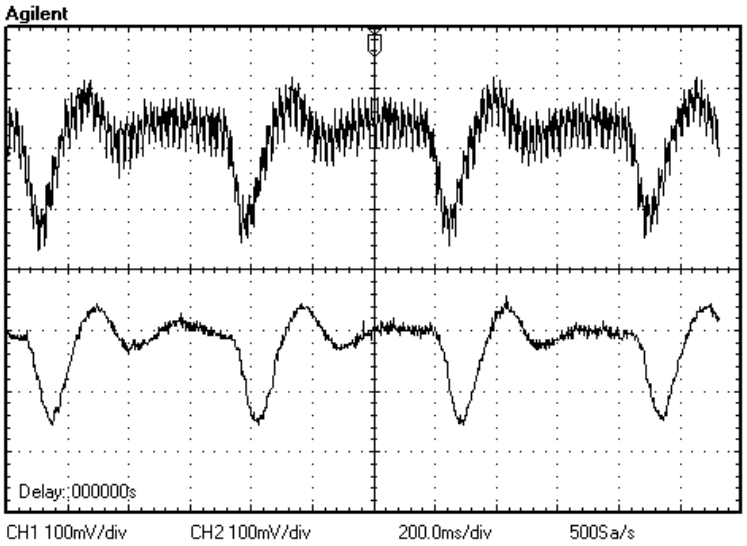


**Fig. 11.** PPG signal corrupted with 50 Hz noise (up) and filtering output (down)

### 5.2. Quantitative Analysis

In addition to the qualitative analysis, the proposed algorithms are evaluated against five (5) quantitative criteria: calculation time, data memory occupation, power consumption, detection accuracy and SNR. In all cases the MC is clocked by 0.75 MHz and powered by 3.3 V.

The calculation time is considered for floating point forward and inverse Haar Transformations (HTs) and proposed fixed point FST and RST. Table 1 gives the results. It is evident that fixed point implementation is more than two times faster for case of forward transform and more than three times faster for case of inverse transform. This fact allows MC to perform real time sampling and processing till 800 Hz, up to 4 levels, what significantly improves the quality of acquisition as well as detection accuracy.

Table 2 gives the memory occupation for floating point and fixed point implementations. And here, the difference is about two times in favor of fixed point. It should be noted that QRS detector implemented by FST occupies in total 224 bytes of DATA memory (+ 44 absolute), 39 bytes of CONST memory and 2 022 bytes of CODE memory. For the case of “de-noising” it is 302 bytes of DATA memory (+ 33 absolute) and 1902 bytes of CODE memory.

**Table 1.** Calculation times for floating and fixed point transforms

| # of decomposition levels | FST [ms] | RST [ms] | Forward HT [ms] | Inverse HT [ms] |
|---|---|---|---|---|
| 4 | 2,35 | 2,23 | 5,82 | 6,90 |
| 5 | 3,96 | 4,37 | 11,86 | 13,99 |
| 6 | 6,93 | 8,63 | 23,91 | 28,14 |
| 7 | 12,64 | 17,10 | 47,99 | 56,41 |

**Table 2.** Memory occupation, DATA MEMORY, RAM, for floating and fixed point transforms

| # of decomposition levels | FST [bytes] | RST [bytes] | Forward HT [bytes] | Inverse HT [bytes] |
|---|---|---|---|---|
| 4 | 74 | 74 | 138 | 138 |
| 5 | 138 | 138 | 266 | 266 |
| 6 | 266 | 266 | 522 | 522 |
| 7 | 522 | 522 | 1034 | 1034 |

By its nature MSP430x is an ultra low power controller. Additionally, the integer point optimization slightly decreases consumption. QRS detector and filter, implemented in this arithmetic, consumed 319 μA and 315 μA that is about 5% less than in case of floating point calculations, 336 μA, 332 μA.

In order to verify the QRS detection accuracy, the 11.094 heart beats within five characteristic files are observed (MIT-BIH Records 101, 103, 202, 230, 234). The particular detection error rate for each record, $DER_i$, is defined as:

$$DER_i[\%] = 100\left(1 - \frac{NFP + NFN}{TN}\right) \quad (\mathbf{13})$$

where are: *NFP* - number of false positives in $X_i[n]$, *NFN* - number of false negatives in $X_i[n]$ and *TN* - total number of QRS complexes in $X_i[n]$. The averaged accuracy is defined as:

$$ADER[\%] = \frac{1}{5}\sum_{i=1}^{i=5} DER_i\,[\%]\ . \quad (\mathbf{14})$$

First, the files are passed through the wavelet based QRS detector realized in MATLAB by algorithm structure and method of modulus maxima given in [24] with distinction that Mexican hat wavelet is replaced with Haar. Then, the analog ECG signals are feed to the proposed MC's QRS detector. ASCII forms of RR intervals are collected by terminal emulator and then statistically analyzed by MATLAB. The averaged accuracies were 99.47% and 99.06%, respectively. Obviously, the proposed MC detector decreases accuracy for -0.41% what can be considered as negligible.

In order to quantitative estimate "de-noising" technique, the output *SNR*, $SNR_o$, is considered for initial value of *SNR*, $SNR_i$ :

$$SNR_o = 10log\frac{\sum_{i=1}^{N} X(i)^2}{\sum_{i=1}^{N}(X(i) - X_r(i))^2}, \quad (\mathbf{15})$$

$$SNR_i = 10log\frac{\sum_{i=1}^{N} X(i)^2}{\sum_{i=1}^{N} n(i)^2}, \quad (\mathbf{16})$$

where, *X(i)* is the original signal, $X_r(i)$ is "de-noised" signal, *n(i)* noise signal and *N* is the length of the signals.

The ECG signals from above MIT-BIH records are corrupted by 50 Hz noise of different amplitudes and passed through the MATLAB codes of proposed MC's "de-noising" algorithm and algorithm based on HT with hard thresholding from [22]. The results are shown in Table 3.

**Table 3.** $SNR_o$ values for "de-noising" algorithms

| $SNR_i$ | 30dB | 20dB | 10dB | 5dB |
|---|---|---|---|---|
| $SNR_o$ – HT | 32.5601 | 23.2341 | 13.5353 | 8.6026 |
| SNRo – Proposed alg. | 31.9473 | 22.7246 | 13.2348 | 8.3626 |
| Improvement - Degradation [%] | -1.8821 | -2.1929 | -2.2201 | -2.7899 |

As can be noted, the classical HT with hard thresholding has better *SNRo*. However, the degradation for proposed algorithm, even in the worst case, is negligible, less than 2.8%.

## 6. Conclusion

Wavelet transforms can be successfully used to solve many tasks in biomedical signal processing. After certain optimizations in the terms of fixed point arithmetic, they can be implemented in low-cost general purpose microcontrollers. Case studies for real-time QRS detection and ECG and PPG "de-noising", implemented in MSP430F169, are presented. The benefits are obvious, 800 Hz sampling rate, 2-4 times faster calculation, less than 500 bytes of data memory occupation, 1 mW power consumption, 99.06% detection accuracy, 5% decreased power consumption and satisfied SNR. The degradations are negligible about -0.41% in accuracy and -2.8%, in SNR. The same approach can be applied with other signals where the embedded implementation of wavelets can be beneficial.

**Acknowledgment.** This paper presents a part of the research performed in the projects: "Development and implementation of embedded systems for medical applications", MESI, supported by Ministry of Science of Montenegro, "Application of Biomedical Engineering in Preclinical and Clinical Practice", III-41007, supported by

the Serbian Ministry of Science and Technology and TEMPUS, 530417-TEMPUS-1-2012-1-UK-TEMPUS-JPCR, “Studies in Bioengineering and Medical Informatics”, supported by EU Commission. The authors are grateful for their support.

## References

1. Graps, A.: An Introduction to Wavelets. Computing in Science and Engineering, Vol. 2, No. 2, IEEE press, 50-61. (1995)
2. Makris, C.: Wavelet trees: a survey. Computer Science and Information Systems, Vol. 9, No. 2, 585-625. (2012)
3. Merry, R.J.E.: Wavelet theory and applications: a literature study. Technische Universiteit Eindhoven (Eindhoven), DCT 2005.053. (2005) [Online]. Available: http://alexandria.tue.nl/repository/books/612762.pdf
4. Zhao, J., Zhang, Z., Han, S., Qu, C., Yuan, Z., Zhang, D.: SVM Based Forest Fire Detection Using Static and Dynamic Features. Computer Science and Information Systems, Vol. 8, No. 3, 821-841. (2011)
5. Addison, P.S.: Wavelet transforms and the ECG: a review. Physiological Measurements, Vol. 26, 155–199. (2005)
6. Texas Instruments Home Page, [Online]. Available: http://www.ti.com/lsds/ti/microcontroller/16-bit_msp430/overview.page?DCMP=MCU_other&HQS=msp430, (January 2012)
7. Vogel, S., Hulsbusch, M., Hennig, T., Blazek, V., Leonhardt, S.: In-Ear Vital Signs Monitoring Using a Novel Microoptic Reflective Sensor. IEEE Trans Inf Technol Biomed, Vol. 13, No. 6, 882-889. (2009)
8. Pantelopoulos, A., Bourbakis, N.G.: A Survey on Wearable Sensor-Based Systems for Health Monitoring and Prognosis. IEEE Transactions on Systems, Man, and Cybernetics, Part C: Applications and Reviews, Vol. 40, Issue 1, 1-22. (2010)
9. Stojanovic, R., Karadaglic, D.: A LED–LED-based photoplethysmography sensor. Physiol. Meas. Vol. 28, 19-27. (2007)
10. Phyu, M. W., Zheng, Y., Zhao, B., Liu, X., Wang, Y. S.: A Real-Time ECG QRS Detection ASIC Based on Wavelet Multiscale Analysis. In Proceedings of the Solid-State Circuits Conference, A-SSCC 2009*.,* 293-296. (2009)
11. Hoang, T. T., Son, J. P., Kang, Y. R., Kim, C. R., Chung, H. Y., Kim, S. W.: A Low Complexity, Low Power, Programmable QRS Detector Based on Wavelet Transform for Implantable Pacemaker. In Proceedings of the 19th IEEE System on Chip Conference (SOCC), Texas, USA, 160-163. (2006)
12. Chio, I. I., Mang, I. V., Peng, U. M.: ECG QRS Complex Detection with Programmable Hardware. In Proceedings *of* the 30th Annual International Conference of the IEEE Engineering in Medicine and Biology Society, Vancouver, British Columbia, Canada, 2920-2923. (2008)
13. Stojanović, R., Karadaglić, D., Mirković, M., Milošević, D.: A FPGA system for QRS complex detection based on Integer Wavelet Transform. Measurement Science Review, Vol. 11, Issue 4, 131-138. (June 2011)
14. Bahoura, M., Hassani, M., Hubin, M.: DSP Implementation of Wavelet Transform for Real Time ECG Wave Forms Detection And Heart Rate Analysis. Computer Methods and Programs in Biomedicine, Vol. 52, 35-44. (1997)
15. Rudnicki, M., Strumillo, P.: A Real-Time Adaptive Wavelet Transform-Based QRS Complex Detector. In proceeding of 8th International Conference on

Adaptive and Natural Computing Algorithms, ICANNGA 2007, Proceedings, Part II, Warsaw, Poland, 281-289. (2007)
16. Kumar, P., Jain, M., Chandra, S.: Low Cost, Low Power QRS Detection Module Using PIC. In Proceedings of the 2011 International Conference on Communication Systems and Network Technologies, Katra, Jammu, India, 414-418. (2011)
17. Mallat, S.G.: A theory for multiresolution signal decomposition: the wavelet representation. IEEE Trans. Pattern Analysis and Machine Intelligence, Vol. 11, No. 7, 674-693. (1989)
18. Calderbank, A.R., Daubechies, I., Sweldens, W., Yeod, B.L.: Wavelet Transforms That Map Integers to Integers. Applied and Computational Harmonic Analysis, Vol. 5, Issue 3, 332-369. (1998)
19. Li, C., Zheng, C., Tai, C.: Detection of ECG characteristic points using wavelet transform. IEEE Transactions on Biomedical Engineering, Vol. 42, Issue 1, 21-28. (1995)
20. Almeida, R., Martinez, J.P., Olmos, S., Rocha, A.P., Laguna, P.: A wavelet-based ECG delineator: Evaluation on standard databases. IEEE Transactions on Biomedical Engineering, Vol. 51, No. 4, 570-581. (2004)
21. Thakor, N.V., Webster, J.G., Tompkins, W.J.: Estimation of QRS complex power spectra for design of a QRS filter. IEEE Trans Biomed Eng., Vol. 31, Issue 11, 702-706. (1984)
22. Šindelářová, I., Ptáček, J., Procházka, A.: Wavelet Transform in Signal De-Noising. Proc. of the 5th Int. Conf. Process Control 2002, R190/1-7. (2002)
23. National Instruments, NI ELVIS II Series Specifications, [Online]. Available: http://www.ni.com/pdf/manuals/372590b.pdf, (January 2012)
24. Romero Legarreta, I., Addison, P.S., Grubb, N.: R-wave Detection Using Continuous Wavelet Modulus Maxima. Computers in Cardiology, Vol. 30, 565−568. (2003)

**Radovan Stojanović** received his M.Sc. from University of Montenegro, in 1990, and Ph.D. from University of Patras, Greece, in 2001. He is currently associate professor at the University of Montenegro. His research interests include embedded systems, applied image and signal processing, instrumentation and measurements, industrial electronics, biomedical engineering. He is an author or cooauthor of more than 150 research papers as well as a coorinator of numerous international, bilateral and national projects. He is a member of the IEEE, associate fellow of IIAS, visiting researcher and lecturer at several EU universities and institutes end founder of Mediteranian Embedded Comupting (MECO) events.

**Saša Knežević** is currently M.Sc. student at Faculty of Electrical Engineering of University of Montenegro. He graduated in 2011 at the Department for Electronics at Faculty of Electrical Engineering of University of Montenegro. His research interests are embedded systems, CAD and software engineering.

**Dejan Karadaglić**, DPhil (Oxon), CEng, MIET, CPhys, MInstP, is a Lecturer at the School of Engineering and Built Environment, Glasgow Caledonian University. His research interests are focused at sensors and imaging area with broad range application, but primarily using optoelectronic techniques in biomedical engineering. He worked at the Universities of Oxford, St Andrews, Liverpool and Manchester in past, where participated in a number of leading-edge technology projects, and published a number of peer-reviewed publications.

**Goran Devedžić** is professor at Faculty of Engineering, University of Kragujevac, Serbia. His research interests focus on the advanced product and process development, industrial and medical application of soft computing techniques, and bioengineering. He has authored/co-authored more than 100 research papers, published in international and national journals or presented at international and national conferences, as well as three books on CAD/CAM technology and 3D product modeling.

*Received: May 17, 2011; Accepted: November 23, 2012.*